HHS Public Access

Author manuscript

Gut. Author manuscript; available in PMC 2021 June 01.

Published in final edited form as:

Gut. 2021 June ; 70(6): 1010–1013. doi:10.1136/gutjnl-2020-322945.

Multiplexed endoscopic imaging of Barrett's neoplasia using targeted fluorescent heptapeptides in a phase 1 proof-of-concept study

Jing Chen[1], **Yang Jiang**[2], **Tse-Shao Chang**[3], **Bishnu Joshi**[1], **Juan Zhou**[1], **Joel H. Rubenstein**[1], **Erik J. Wamsteker**[1], **Richard S. Kwon**[1], **Henry D. Appelman**[4], **David G. Beer**[5], **D. Kim Turgeon**[1], **Eric J. Seibel**[6], **Thomas D. Wang**[1,3,7,*]

[1]Division of Gastroenterology, Department of Internal Medicine, University of Michigan, Ann Arbor, MI 48109, USA

[2]Department of Bioengineering, University of Washington, Seattle, WA 98195, USA

[3]Department of Mechanical Engineering, University of Michigan, Ann Arbor, MI 48109, USA

[4]Department of Pathology, University of Michigan, Ann Arbor, MI 48109, USA

[5]Department of Surgery, Section of Thoracic Surgery, University of Michigan, Ann Arbor, MI 48109, USA

[6]Department of Mechanical Engineering, University of Washington, Seattle, WA 98195, USA

[7]Department of Biomedical Engineering, University of Michigan, Ann Arbor, MI 48109, USA

Message

Imaging molecular expression patterns may improve methods for early cancer detection in patients with Barrett's esophagus (BE). A multiplexed strategy that detects two targets simultaneously is demonstrated. Heptapeptides specific for EGFR and ErbB2 were labeled with Cy5 and IRDye800, respectively. Fluorescence images from n = 22 BE patients were collected in vivo using a multi-modal scanning fiber endoscope. The images were evaluated using support vector machine and logistic regression methods, and revealed 92% sensitivity and 89% specificity. This first-in-human pilot study demonstrates feasibility to detect multiple targets concurrently and potential for early detection of cancers that are molecularly heterogeneous.

[*]**Corresponding author:** Thomas D. Wang, M.D., Ph.D. Professor of Internal Medicine, Biomedical Engineering, and Mechanical Engineering, Division of Gastroenterology, University of Michigan, 109 Zina Pitcher Pl. BSRB 1522, Ann Arbor, MI 48109-2200, Office: (734) 936-1228, Fax: (734) 647-7950, thomaswa@umich.edu.

Contributors JC, BPJ, JZ, DGB, DKT, EJS, and TDW conceived and designed the experiments. JC, TSC, JHR, EJW, and RSK performed the experiments. JHR, YJ, EJS contributed to image and data analysis. HDA reviewed pathology. JC, YJ, EJS, and TDW wrote the manuscript.

Competing interests BPJ, JZ, TDW are the inventors on patents filed by the University of Michigan on the peptides presented in this study. EJS is an inventor of the mmSFE technology, and participates in the royalty sharing program for patents owned by the University of Washington. The remaining authors disclose no conflicts.

Patient consent for publication Not required.

Keywords

imaging; Barrett's esophagus; peptides; targets

BACKGROUND

Esophageal adenocarcinoma (EAC) is a deadly disease that has increased dramatically in incidence.[1,2] Endoscopic screening with white light illumination and random biopsy is limited by sampling error.[3] Dysplasia often presents with flat architecture and patchy distribution.[4] EGFR and ErbB2 are transmembrane tyrosine kinase receptors that stimulate epithelial cell growth, proliferation, and differentiation.[5] Overexpression of these targets reflects a higher risk for cancer progression.[6–8] Multiplexed imaging methods take advantage of the broad spectrum of light over the visible and near-infrared (NIR) regime. We aim to demonstrate clinical feasibility to visualize EGFR and ErbB2 expression simultaneously in vivo to detect Barrett's neoplasia.

METHODS

Consecutive patients referred for either evaluation or therapy of Barrett's neoplasia were recruited for the study (NCT03589443). A multi-modal scanning fiber endoscope (mmSFE) was designed to collect two fluorescence images concurrently. Target/background (T/B) ratios were calculated for each fluorescence image. Details are provided online in Supplementary file.

RESULTS

The peptide QRHKPRE specific for EGFR was labeled with Cy5 via a GGGSK linker, Figure 1A,[9] and KSPNPRF, specific for ErbB2, was labeled with IRDye800 via a GGGSC linker, Figure 1B.[10] These fluorophores were chosen to minimize overlap between absorbance and emission spectra, Figure 1C. The characteristics and stability of fluorescently labeled peptides are shown, Table S1-S4. The pharmacology/toxicology study showed no acute adverse effects in animals for either peptide, Table S5,6. A Phase 1 safety study performed in n = 25 human showed no abnormalities in the laboratory results, urinalysis, and EKG for either peptide, and no adverse events (AE) were found.

The mmSFE was designed to collect multiplexed fluorescence images, Figure 1D-H. Contrast agents were administered, and real time images were collected from n = 22 subjects, Table 1 (Videos S1-23). Representative white light images are shown for squamous (SQ) and non-dysplastic BE (NDBE), Figures 2A,B. Minimal background was seen following peptide administration. Fluorescence images were collected in separate channels, and co-registered reflectance provided anatomic landmarks for image interpretation. A representative set of in vivo images for HGD and EAC is shown, Figures 2C,D. Increased fluorescence intensities were seen from regions of HGD and EAC, and were confirmed by pathology. Immunohistochemistry (IHC) was performed to validate EGFR and ErbB2 expression on excised specimens, Figure S1.

The T/B ratios using QRH*-Cy5 and KSP*-IRDye800 were measured from individual patients, and are shown, Figure 3A,B. For SQ (n = 2) or NDBE (n = 3), a mean (±SD) T/B ratio of 1.28±0.07 for QRH*-Cy5 and 1.33±0.15 for KSP*-IRDye800, respectively, was calculated. The T/B for (n = 4) LGD was 1.23±0.05 and 1.18±0.10, respectively. For HGD (n=7) and EAC (n = 6), a mean (±SD) T/B ratio of 1.61±0.21 and 1.68±0.24, respectively, was found. Leave-one-out cross-validation (LOOCV) was used to classify results, Table S7. Support vector machine (SVM) and logistic regression (LR) provided the highest classification accuracy of 91%. The imaging results revealed n = 12, 1, 8, and 1 true positives, false positives, true negatives, and false negatives, respectively, resulting in 92% sensitivity and 89% specificity. The decision boundaries using SVM and LR are shown. The ROC curves using these methods with LOOCV are displayed, Figure 3C. A higher AUC was achieved with multiplexed detection versus either target alone from bootstrap, Figure 3D.

COMMENTS

Here, we demonstrate feasibility to detect Barrett's neoplasia endoscopically by imaging two targets concurrently in vivo. Fluorescently labeled peptides specific for EGFR and ErbB2 were administered topically in the distal esophagus of n = 22 BE patients. With conventional white light illumination, structural abnormalities associated with Barrett's neoplasia appeared subtle. By comparison, spatial patterns of target expression were visualized with high contrast using fluorescence. Two laser excitation wavelengths were delivered concurrently through a single flexible optical fiber using a prototype wide-field endoscope accessory. Adequate signal was collected by using large core, high numerical aperture fibers. The regions imaged were compared with histopathology of specimens excised via either EMR or biopsy. Immunohistochemistry of these specimens confirmed heterogeneous expression of EGFR and ErbB2.

To our knowledge, this study is the first to demonstrate clinical application of multiplexed imaging during endoscopy. Many cancers, such as EAC, are molecularly heterogeneous, thus the capacity to detect multiple targets concurrently may result in more accurate clinical diagnosis. Mucosal abnormalities with non-specific features, such as nodularity, ulceration, and irregularity, are not specific for accurate location of Barrett's neoplasia. Leading medical societies recommend random 4-quadrant biopsies for EAC surveillance, but this sampling method is inefficient and has been poorly adopted by community physicians.[11] Molecular biomarkers can be highly specific for disease, and are expressed before neoplastic lesions become grossly apparent. Endoscopic imaging strategies for detecting these targets in vivo can be used to guide and prioritize high risk regions for resection, reduce surveillance frequency, and minimize over diagnosis.

Recently, detection of dysplasia and early EAC in BE patients was demonstrated using an antibody specific for vascular endothelial growth factor A (VEGFA). Bevacizumab was originally developed for cancer therapy, and was repurposed for diagnostic imaging by labeling with IRDye800.[12] Compared with antibodies, peptides are much smaller in size, have faster binding kinetics, and can be mass manufactured at lower costs.[13–15] The peptides were delivered topically to the mucosal surface in the distal esophagus. This method was effective for staining regions of neoplastic BE involvement.[16] Compared with systemic

delivery, this approach localizes the distribution of exogenous imaging agents to the target tissues only, minimizes background, and maximizes image contrast. This strategy could be performed because the peptides used have similar binding kinetics.[9,10] Lectins have been investigated for detection of Barrett's neoplasia ex vivo,[17] but have not been demonstrated clinically. Fluorescently-labeled peptides for targeted detection of pre-malignant lesions in the colon have also been shown clinically.[18,19] Folate has been developed for targeted imaging of ovarian cancer,[20] however, small molecules have limited flexibility for fluorescence labeling and would be difficult to arrange for multiplexed imaging.

In this work, light over a broad optical spectrum was collected using a flexible fiber endoscope accessory, and was separated into fluorescence and reflectance channels.[21] Multi-pixel photon counters with much higher sensitivity than the charge-coupled devices (CCD) found in video endoscopes were used. Multiplexed detection was achieved by exciting Cy5 and IRDye800 at wavelengths with minimal overlap between the absorption and emission bands. Additional targets can be detected by extending this strategy to the full visible and NIR spectrum.[22] Fluorescence emission in the NIR regime mitigates the effects of hemoglobin absorption and tissue scattering, and minimizes tissue autofluorescence background.[23] The distal optics and scan strategy used provide much greater spatial resolution than an optical fiber bundle.

The clinical usefulness of this technology can be improved by addressing several study limitations. The peptides were administered separately to minimize potential binding interactions but can be combined to reduce time needed to reconstitute and prepare the peptides for delivery. After inserting the mmSFE accessory through the working channel, the fluorescence and HD-WLE images were not registered. Accurate alignment would allow the fluorescence images to be more effective as a real-time guide for tissue resection. This study was performed at a tertiary referral center that specializes in treatment of patients with advanced BE, thus a cohort highly enriched with neoplasia was studied. Inclusion of more non-neoplastic subjects would better reflect the prevalence of disease seen in the community. In conclusion, we demonstrated proof-of-concept for detecting multiple targets concurrently in patients with Barrett's neoplasia and promise for this strategy to detect cancers in hollow organs early.

Supplementary Material

Refer to Web version on PubMed Central for supplementary material.

Acknowledgements

We thank E Brady, D Chandhrasekhar, and A Cawthon for clinical support, and BR Reisdorph for regulatory support.

Funding This study was supported in part by the National Institutes of Health U54 CA163059 (DGB, JHR, EJS, TDW), U01 CA189291 (TDW) and R01 CA200007 (EJS, TDW).

Abbreviations –

BE	Barrett's esophagus

SQ	squamous
LGD	low grade dysplasia
HGD	high grade dysplasia
EAC	esophageal adenocarcinoma
mmSFE	multi-modal scanning fiber endoscope
NIR	near infrared

REFERENCES

1. Thrift AP, Whiteman DC. The incidence of esophageal adenocarcinoma continues to rise: analysis of period and birth cohort effects on recent trends. Ann Oncol 2012;23:3155–62. [PubMed: 22847812]
2. Siegel RL, Miller KD, Jemal A. Cancer statistics. CA Cancer J Clin 2016;66:7–30. [PubMed: 26742998]
3. Sharma P, Savides TJ, Canto MI, et al. The american society for gastrointestinal endoscopy PIVI (preservation and incorporation of valuable endoscopic innovations) on imaging in Barrett's esophagus. Gastrointest Endosc 2012;76:252–4. [PubMed: 22817781]
4. Spechler SJ, Sharma P, Souza RF, et al. American gastroenterological association medical position statement on the management of Barrett's esophagus. Gastroenterology 2011;140:1084–91. [PubMed: 21376940]
5. Citri A, Yarden Y. EGF-ERBB signalling: towards the systems level. Nat Rev Mol Cell Biol 2006;7:505–16. [PubMed: 16829981]
6. Dulak AM, Schumacher SE, van Lieshout J, et al. Gastrointestinal adenocarcinomas of the esophagus, stomach, and colon exhibit distinct patterns of genome instability and oncogenesis. Cancer Res 2012;72:4383–93. [PubMed: 22751462]
7. Dulak AM, Stojanov P, Peng S, et al. Exome and whole-genome sequencing of esophageal adenocarcinoma identifies recurrent driver events and mutational complexity. Nat Genet 2013;45:478–86. [PubMed: 23525077]
8. Miller CT, Moy JR, Lin L, et al. Gene amplification in esophageal adenocarcinomas and Barrett's with high-grade dysplasia. Clin Cancer Res 2003;9:4819–25. [PubMed: 14581353]
9. Zhou J, Joshi BP, Duan X, et al. EGFR overexpressed in colonic neoplasia can be detected on wide-field endoscopic imaging. Clin Transl Gastroenterol 2015;6:e101.
10. Joshi BP, Zhou J, Pant A, et al. Design and synthesis of near-infrared peptide for in vivo molecular imaging of HER2. Bioconjug Chem 2016;27:481–94. [PubMed: 26709709]
11. Kariv R, Plesec TP, Goldblum JR, et al. The seattle protocol does not more reliably predict the detection of cancer at the time of esophagectomy than a less intensive surveillance protocol. Clin Gastroenterol Hepatol 2009;7:653–8. [PubMed: 19264576]
12. Nagengast WB, Hartmans E, Garcia-Allende PB, et al. Near-infrared fluorescence molecular endoscopy detects dysplastic oesophageal lesions using topical and systemic tracer of vascular endothelial growth factor A. Gut 2019;68:7–10. [PubMed: 29247063]
13. Lee S, Xie J, Chen X. Peptides and peptide hormones for molecular imaging and disease diagnosis. Chem Rev 2010;110:3087–111. [PubMed: 20225899]
14. Wu AM, Senter PD. Arming antibodies: prospects and challenges for immunoconjugates. Nat Biotechnol 2005;23:1137–46. [PubMed: 16151407]
15. Conner KP, Rock BM, Kwon GK, et al. Evaluation of near infrared fluorescent labeling of monoclonal antibodies as a tool for tissue distribution. Drug Metab Dispos 2014;42:1906–13. [PubMed: 25209366]
16. Sturm MB, Joshi BP, Lu S, et al. Targeted imaging of esophageal neoplasia with a fluorescently labeled peptide: first-in-human results. Sci Transl Med 2013;5:184ra161.

17. Bird-Lieberman EL, Neves AA, Lao-Sirieix P, et al. Molecular imaging using fluorescent lectins permits rapid endoscopic identification of dysplasia in Barrett's esophagus. Nat Med 2012;18:315–21. [PubMed: 22245781]

18. Burggraaf J, Kamerling IMC, Gordon PB, et al. Detection of colorectal polyps in humans using an intravenously administered fluorescent peptide targeted against c-Met. Nat Med 2015;21:955–61. [PubMed: 26168295]

19. Joshi BP, Dai Z, Gao Z, et al. Wide-field endoscopic imaging of sessile serrated adenomas with fluorescently-labeled peptide probe. Gastroenterology 2017;152:1002–13. [PubMed: 28012848]

20. van Dam GM, Themelis G, Crane LMA, et al. Intraoperative tumor-specific fluorescence imaging in ovarian cancer by folate receptor-α targeting: first in-human results. Nat Med 2011;17:1315–9. [PubMed: 21926976]

21. Savastano LE, Zhou Q, Smith A, et al. Multimodal laser-based angioscopy for structural, chemical, and biological imaging of atherosclerosis. Nat Biomed Eng 2017;1:0023. [PubMed: 28555172]

22. Miller SJ, Joshi B, Wang TD, et al. Targeted detection of murine colonic dysplasia in vivo with flexible multispectral scanning fiber endoscopy. J Biomed Opt 2012;17:021103.

23. Ntziachristos V, Bremer C, Weissleder R. Fluorescence imaging with near-infrared light: new technological advances that enable in vivo molecular imaging. Eur Radiol 2003;13:195–208. [PubMed: 12541130]

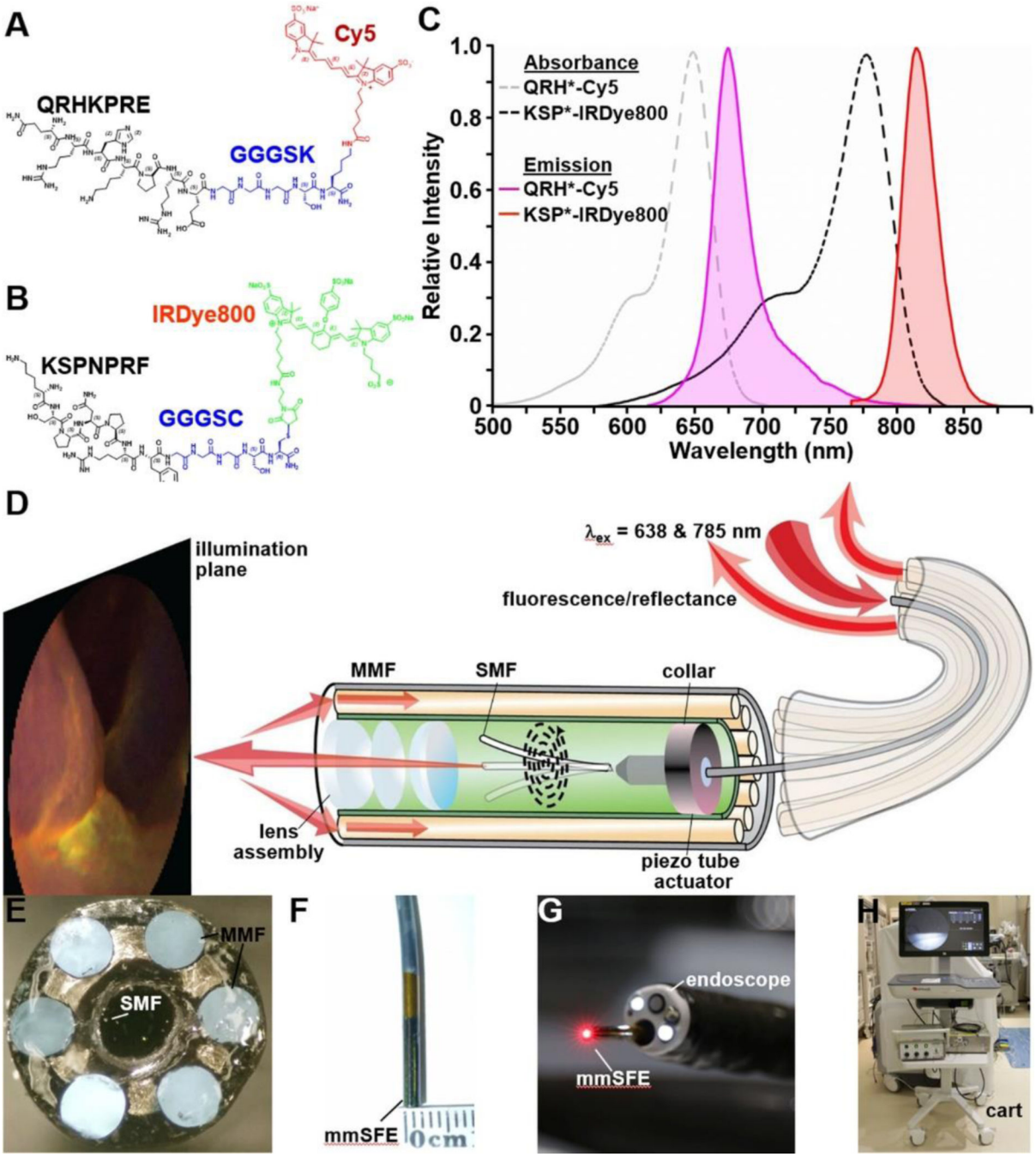

Figure 1. Fluorescently labeled peptides for multiplexed imaging.

Biochemical structures are shown for **A**) QRH*-Cy5, and **B**) KSP*-IRDye800. **C**) Peak absorbance of QRH*-Cy5 and KSP*-IRDye800 occurs at λ_{abs} = 648 and 776 nm, respectively. Peak fluorescence emits at λ_{em} = 675 and 812 nm, respectively. **D**) Schematic diagram for the multi-modal scanning fiber endoscope (mmSFE) is shown. Excitation at λ_{ex} = 638 and 785 nm is delivered through a single-mode fiber (SMF) that is scanned in a spiral pattern by a piezo tube actuator. The beam is focused onto the tissue surface (illumination plane) by a compact lens assembly. **E**) Fluorescence is collected by a ring of large core

multi-mode fibers (MMF) mounted around the instrument periphery. **F**) The dimensions of the rigid tip are 9 mm in length and 2.4 mm in diameter. **G**) This instrument passes forward through the 2.7 mm diameter working channel of a standard medical endoscope (Olympus #GIF-HQ190). **H**) The system is contained within a portable cart.

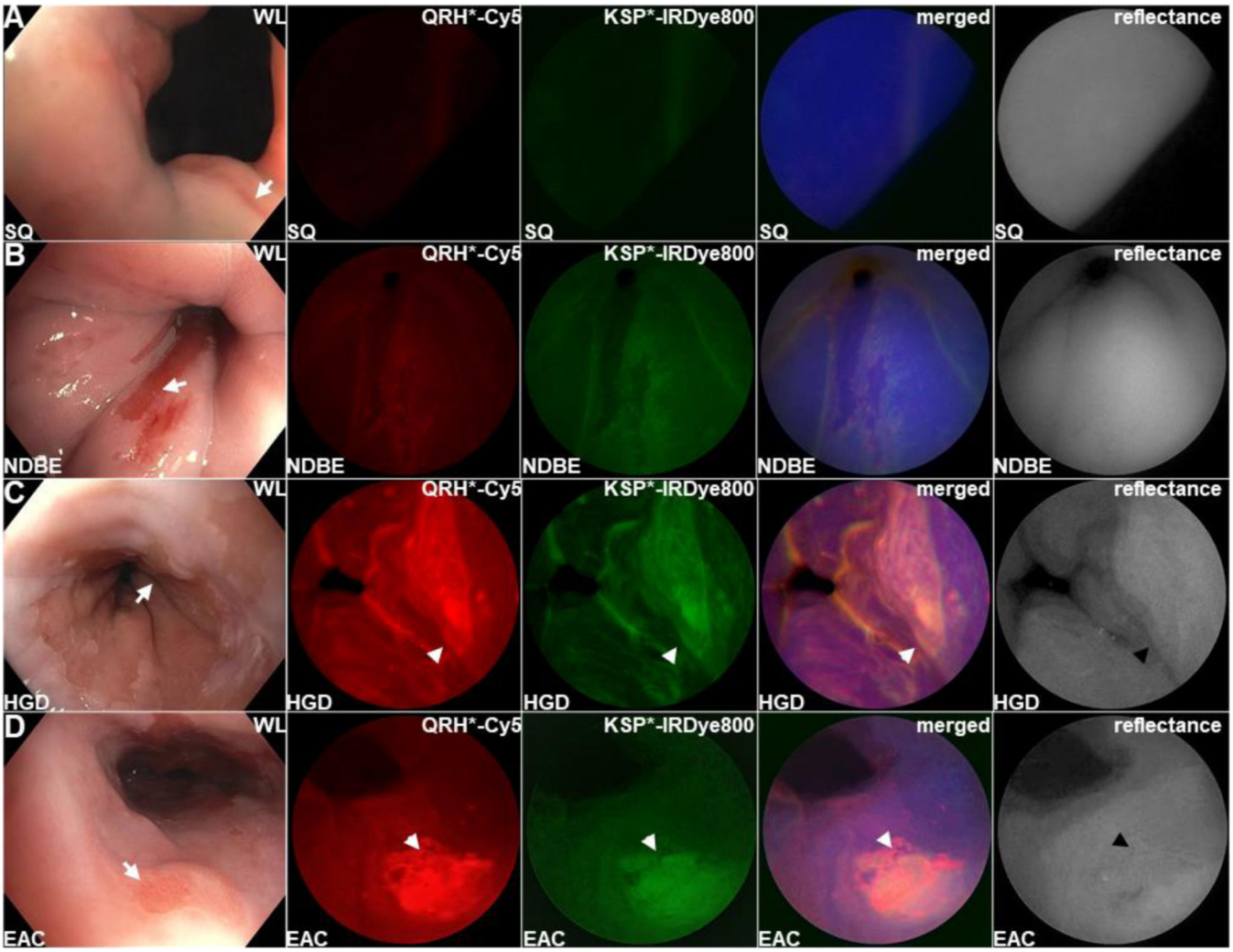

Figure 2. Barrett's esophagus.

Representative in vivo images collected endoscopically are shown from patients with (**A**) squamous (SQ), (**B**) non-dysplastic Barrett's esophagus (NDBE), (**C**) high grade dysplasia (HGD), and (**D**) esophageal adenocarcinoma (EAC). The presence of NDBE is identified by salmon red patches (arrows) in the white light images. Fluorescence images are collected after topical administration of QRH*-Cy5 and KSP*-IRDye800 separately. The merged images show high contrast regions-of-interest (ROIs) where EGFR and ErbB2 (orange) are co-expressed. Co-registered reflectance images provide anatomical landmarks to help interpret the location of the ROIs.

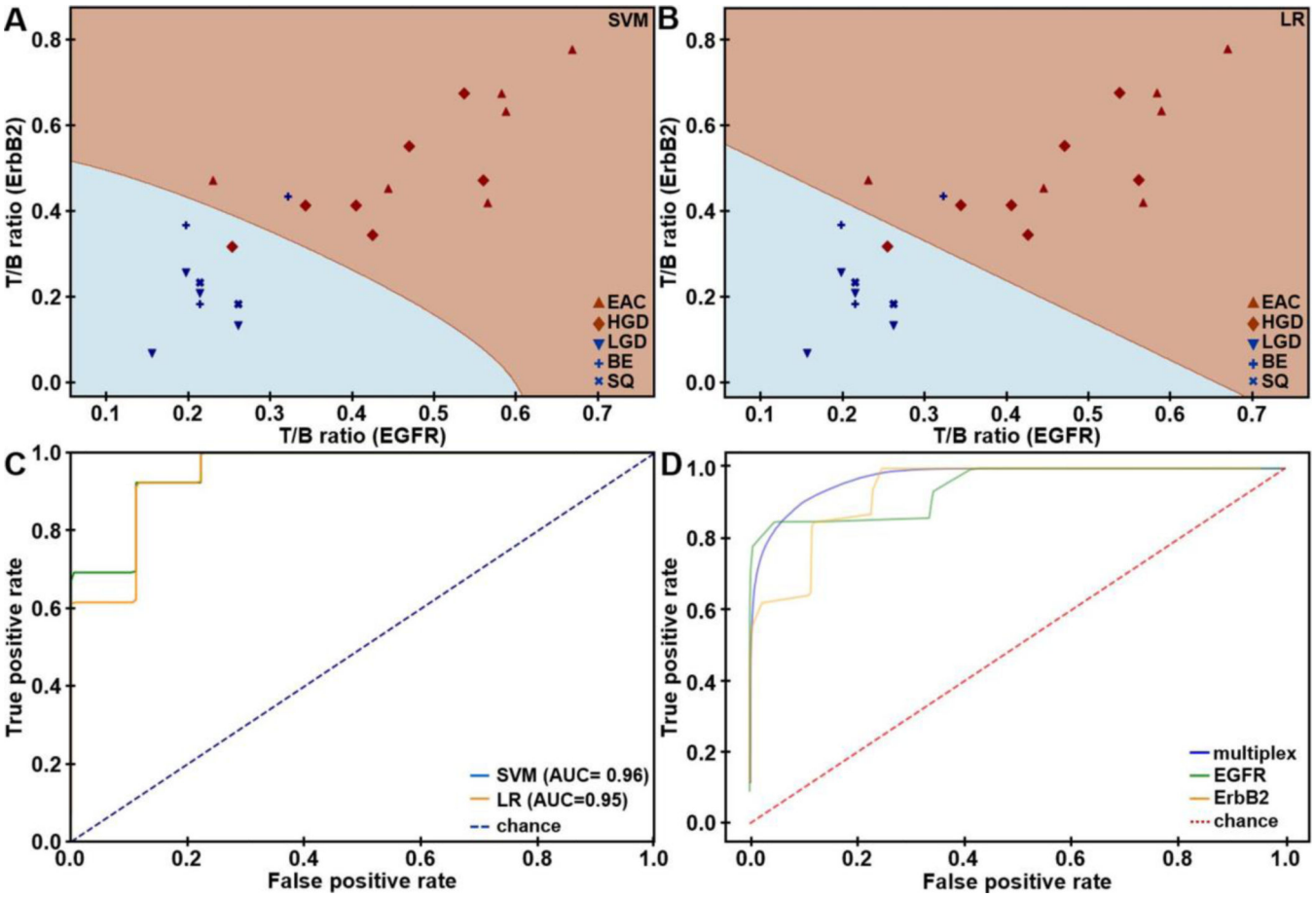

Figure 3. In vivo imaging performance.

Scatter plots show T/B ratios measured for EGFR and ErbB2 expression in the fluorescence images collected in vivo from the distal esophagus of n = 22 patients. Decision boundaries show regions classified as either negative (blue) or positive (brown) for neoplasia using **A**) support vector machine (SVM) and **B)** logistic regression (LR) trained on all data. **C)** ROC curves for classifying HGD/EAC from SQ/NDBE/LGD are shown using SVM and LR algorithms with leave-one-out cross-validation (LOOCV). **D**) Average ROC curves from bootstrap using SVM (AUC = 0.97) model trained on all data show that multiplexed detection provides improved performance than using either EGFR (AUC = 0.95) or ErbB2 alone (AUC = 0.94).

Table 1

Patient demographics.

Multiplexed images were collected in vivo from the distal esophagus of n = 22 patients with a mean (±SD) age of 70.0±10.8 years. Squamous (SQ), non-dysplastic Barrett's esophagus (NDBE), and low-grade dysplasia (LGD) were identified in a total of n = 2, 3, and 4 subjects, respectively. High-grade dysplasia (HGD) and esophageal adenocarcinoma (EAC) were found in n = 7 and 6 subjects, respectively. Modified Prague classification includes length in centimeters of circumferential Barrett's esophagus (C), maximal tongue (M), and any proximal island (I). These findings were confirmed by histopathology from either endoscopic mucosal resection (EMR) or biopsy.

Age	Gender	Prague/Stage	Tissue Sampling	Pathology
68	M	C0M0I0	EMR/biopsy	SQ
57	M	C0M0I0	biopsy	SQ
84	F	C0M0I9	biopsy	NDBE
60	M	C0M1	EMR/biopsy	NDBE
56	M	C1M3	EMR/biopsy	NDBE
57	M	C7M9	biopsy[a]	LGD
56	F	C0M1	biopsy[a]	LGD
80	F	C0M0I0	biopsy[a]	LGD
67	M	C0M0I7	EMR/biopsy	LGD
79	F	C0M2	biopsy	HGD
88	M	C0M3	EMR/biopsy	HGD
79	M	C0M1I1.5	EMR/biopsy	HGD
85	M	C12M13	biopsy	HGD
79	M	C4M5	biopsy	HGD
66	M	C0M0	biopsy	HGD
60	M	C9M10	biopsy	HGD
75	M	T3N1	biopsy	EAC
73	F	C0M0I2	EMR/biopsy	EAC
81	M	C10M10	biospy[b]	EAC
71	M	C9M12I13	EMR/biopsy	EAC
55	F	T1a	biopsy	EAC
64	F	C0M1	EMR/biopsy	EAC

[a] No tissue sampling performed at time of fluorescence imaging. Pathology based on findings from the most recent pathological reports before and after the imaging procedure.

[b] A mass was found in the thoracic esophagus and the tissue diagnosis was obtained prior to this exam.